

# Realistic Quantitative Descriptions of Electron Transfer Reactions: Diabatic Free-Energy Surfaces from First-Principles Molecular Dynamics

P. H.-L. Sit,<sup>1</sup> Matteo Cococcioni,<sup>2</sup> and Nicola Marzari<sup>2</sup>

<sup>1</sup>*Department of Physics, Massachusetts Institute of Technology, Cambridge, Massachusetts 02139, USA*

<sup>2</sup>*Department of Materials Science and Engineering, Massachusetts Institute of Technology, Cambridge, Massachusetts 02139, USA*

(Received 27 February 2006; published 11 July 2006)

A general approach to calculate the diabatic surfaces for electron-transfer reactions is presented, based on first-principles molecular dynamics of the active centers and their surrounding medium. The excitation energy corresponding to the transfer of an electron at any given ionic configuration (the Marcus energy gap) is accurately assessed within ground-state density-functional theory via a novel penalty functional for oxidation-reduction reactions that appropriately acts on the electronic degrees of freedom alone. The self-interaction error intrinsic to common exchange-correlation functionals is also corrected by the same penalty functional. The diabatic free-energy surfaces are then constructed from umbrella sampling on large ensembles of configurations. As a paradigmatic case study, the self-exchange reaction between ferrous and ferric ions in water is studied in detail.

DOI: [10.1103/PhysRevLett.97.028303](https://doi.org/10.1103/PhysRevLett.97.028303)

PACS numbers: 82.30.Fi, 71.15.Pd, 82.20.Wt, 82.20.Yn

A wide variety of processes and reactions in electrochemistry, molecular electronics, and biochemistry have a common denominator: they involve a diabatic electron-transfer process from a donor to an acceptor [1]. These reactions cover processes and applications as diverse as solar-energy conversion in the early steps of photosynthesis, oxidation-reduction reactions between a metallic electrode and solvated ions, and the  $I$ - $V$  characteristics of molecular-electronics devices [2]. The key quantities of interest are the reaction rates (or, equivalently, the conductance) and the reaction pathways. Reaction rates, in the general scenario of Marcus theory [3–5], have a thermodynamic contribution (the classical Franck-Condon factor, broadly related to the free-energy cost of a nuclear fluctuation that makes the donor and the acceptor levels degenerate in energy), and an electronic structure, tunneling contribution (the Landau-Zener term, related to the overlap of the initial and final states).

We argue in the following that state-of-the-art first-principles molecular dynamics calculations, together with several algorithmic and conceptual advances, are able to describe with quantitative accuracy these diabatic processes, while including the realistic description of the complex environment encountered, e.g., in nanoscale devices or at the interface between molecules and metals.

Figure 1 shows schematically an electron-transfer process and the free-energy diabatic surfaces according to the picture that was pioneered by Marcus [3,4,6,7]. In a polar solvent, the electron-transfer process is mediated by thermal fluctuations of the solvent molecules. In the reactant state, the transferring electron is trapped at the donor site by solvent polarization; transfer might occur when the electron donor and acceptor sites become degenerate due to the thermal fluctuations of the solvent molecules. To characterize the role of the solvent on the electron-transfer reaction, a reaction coordinate  $\epsilon$  for a given ionic configuration is introduced, as the energy difference between the

product and reactant state at that configuration [8]. This definition of reaction coordinate captures the collective contributions from the solvent.

There have been a number of pioneering classical molecular dynamic studies [5,9,10] studying the reactions between aqueous metal ions. However, quantitative agreement has not been achieved with classical force fields. The reorganization energy  $\lambda$  (i.e., the free-energy cost to reorganize the solvent molecules from the configurations at equilibrium with the product to the configurations at equilibrium with the reactant without electron transfer) for the aqueous  $\text{Fe}^{2+}$ - $\text{Fe}^{3+}$  self-exchange reaction was found to be 3.6 eV for ions 5.5 Å apart [10], while experimentally [11] (at the slightly shorter separation of 5.32 Å) it is found to be 2.1 eV. Although there have been studies of electron-transfer reactions including electronic polarization in classical force-field potentials [12,13], full first-principles studies are required to describe realistically and quantitatively these reactions. Recently, an elegant grand-canonical density-functional approach has been introduced to address this class of problems [14,15]. This approach is,

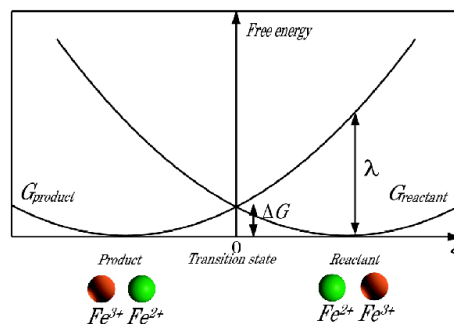


FIG. 1 (color online). Diabatic free-energy surfaces for ferrous-ferric electron-transfer reactions.  $\Delta G$  is the free-energy barrier, and  $\lambda$  is the reorganization energy. The reaction coordinate  $\epsilon$  is the Marcus energy gap.

however, targeted at half reactions for a donor or an acceptor in contact with an electron reservoir.

In this Letter, we present a novel technique to study electron-transfer reactions from first-principles molecular dynamics, with ferrous-ferric self-exchange as a paradigmatic example. We use Car-Parrinello molecular dynamics [16,17] and spin-polarized density-functional theory in the Perdew-Burke-Ernzerhof generalized gradient approximation (PBE-GGA) approximation [18]. Figure 2 shows schematically the sampling procedure used, following the lines of Ref. [10] for classical simulations. An ionic trajectory is first generated with the ions in the  $(2+r)$  and  $(3-r)$  states of charge, respectively.  $r$  is an ‘‘umbrella-sampling’’ parameter used to explore different regions of the phase space. We then perform two separate runs with the electronic state constrained in the reactant or in the product configuration, and with the ions following the afore-generated ionic trajectories. The reaction coordinate  $\epsilon$  at every time step is thus given by the difference between the energies of the product and the reactant state. The probability distribution  $P(\epsilon)$  is then calculated as:

$$P(\epsilon) = \frac{\sum_{\tau} \delta_{\epsilon'(\tau), \epsilon} \exp\{-\beta[E_r(\tau) - E_s(\tau)]\}}{\sum_{\tau} \exp\{-\beta[E_r(\tau) - E_s(\tau)]\}}, \quad (1)$$

where  $\epsilon'(\tau) = E_p(\tau) - E_r(\tau)$  is the reaction coordinate at time  $\tau$ ;  $E_r(\tau)$ ,  $E_p(\tau)$ , and  $E_s(\tau)$  are the energies of the system in the reactant, product, and sampling oxidation states, respectively, at time  $\tau$ , and  $\delta_{\epsilon'(\tau), \epsilon}$  is the Kronecker delta. The exponential term in the expression above restores the correct thermodynamical sampling according to the energy surface  $E_r$ . The free-energy  $G(\epsilon)$  is derived from the probability distribution  $P(\epsilon)$  as  $G(\epsilon) = -k_B T \ln[P(\epsilon)]$ .

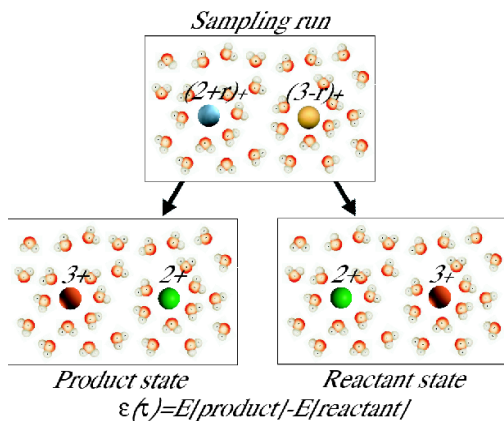


FIG. 2 (color online). Procedure used to calculate the diabatic free-energy surfaces for electron transfer: The reaction coordinate at each time step is calculated from the energy difference between the product and reactant states in the ionic configuration provided by the sampling run. The phase space is explored via the umbrella-sampling parameter  $r$ , determining the oxidation state of the ions.

It is of central importance to note that due to the lack of self-interaction correction in common exchange-correlation functionals, the transferring ( $3d$  minority-spin) electron will unphysically split between the two ions. Moreover, to calculate the energy gap, we need to accurately calculate the total energy when the minority-spin electron localizes at either reactant or product site at any given ionic configuration.

In order to address these central problems, we first consider the simple case when oxidation states can be controlled trivially. This happens when two ions are infinitely apart; the two ions can be studied in separate simulation cells and the oxidation states are controlled by simply changing the total number of electrons. For this special case, we performed runs using  $\text{Fe}^{(2+r)+}$  and  $\text{Fe}^{(3-r)+}$  (with  $r = 0.0, 0.25, 0.50, 0.75$ , and  $1.0$ ), each solvated with 31 water molecules in the unit cell. We then carried out one  $\text{Fe}^{2+}$  and one  $\text{Fe}^{3+}$  run in the trajectory generated with  $\text{Fe}^{(2+r)+}$ , and one  $\text{Fe}^{2+}$  and one  $\text{Fe}^{3+}$  run in the trajectory generated with  $\text{Fe}^{(3-r)+}$ . [When calculating energies of charged systems in periodic-boundary conditions, the Coulomb interaction of charges with their periodic images should be removed [19]. In practice, these errors cancel out when calculating the energy gap, which is the difference in energy between systems with the same charge.]

Figure 3 shows the resulting diabatic surfaces; the final result is obtained by integrating [20]

$$F(\epsilon) = \frac{\sum_r F_r(\epsilon) g_r(\epsilon)}{\sum_r g_r(\epsilon)}, \quad (2)$$

where  $F_r(\epsilon)$  is the slope of the free-energy curve in the different sections, each characterized by an umbrella-sampling parameter  $r$ , and the weighting factor  $g_r(\epsilon) = \langle \delta(\epsilon - \epsilon(\tau)) \rangle_r$ . Each simulation lasted 5 ps after accurate thermalization. For this special case, the trajectories gen-

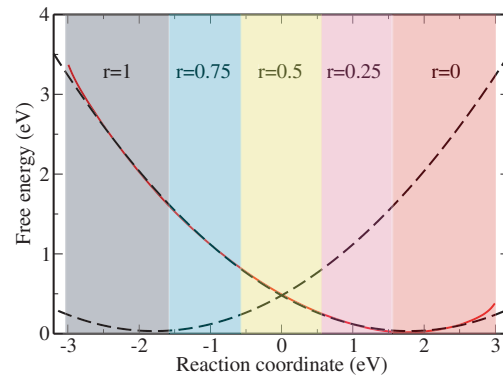


FIG. 3 (color online). Diabatic free-energy surface for ferrous-ferric electron transfer in the special case when two ions are infinitely apart. The solid curve has been obtained from first-principles molecular dynamics. The dashed curves are mirror images, and correspond to a parabolic fit of the data. Different shades indicate portions of the diabatic surface sampled with  $r = 0, 0.25, 0.5, 0.75$ , and  $1$ .

erated with  $\text{Fe}^{(2+r)+}$  and  $\text{Fe}^{(3-r)+}$  are independent; since each of them provides  $n$  data points, there will be  $n^2$  energy gaps, providing high statistics and a very smooth free-energy curve that fits accurately a parabola, with a coefficient of determination ( $R^2$ ) of 0.9996, and a reorganization energy of 1.77 eV.

As mentioned earlier, the self-interaction errors of most exchange-correlation functionals result in a dramatic qualitative failure in describing ions in different oxidation states when more than one ion is present. This failure can be exemplified by the case of two iron ions in the 2+ and 3+ oxidation state. When such a system is studied—e.g. using PBE-GGA—the highest occupied molecular orbital (HOMO) electron will split between the two iron centers, to decrease its own self-interaction. This behavior takes place irrespective of the chemical environment of the two iron centers; we observe it for two isolated atoms, two hexa-aqua iron complexes, or two ions fully solvated.

We will show in the following that this failure can be corrected by adding a penalty cost to ground states with noninteger occupation of the ion centers [21]. This same approach is also used to calculate the Marcus energy gap, where for a given configuration we need to determine both the correct ground-state energy (with the transferring electron in the reactant electronic configuration) and the first excited state (with the transferring electron in the product electronic configuration). We use and validate the following penalty functional

$$E[\{\psi_i\}] \rightarrow E[\{\psi_i\}] + \sum_I \frac{P^I}{\sigma_I \sqrt{2\pi}} \int_{-\infty}^{f_0^I - f_{\{\psi_i\}}^I} \exp\left(-\frac{x^2}{2\sigma_I^2}\right) dx, \quad (3)$$

where  $f_{\{\psi_i\}}^I$  is the largest eigenvalue of the minority-spin occupation matrix on ion  $I$  (calculated in this work by projecting the minority-spin Kohn-Sham orbitals on the  $3d$  orbitals of an isolated iron atom), and  $f_0^I$  is its target value. To determine the optimal parameters, we separately calculated the minority-spin occupation matrix for either a ferrous or ferric hexa-aqua ion embedded in a dielectric continuum ( $\epsilon = 78$ ) [22]. Then, we determine the parameters in the penalty functional so that the occupation matrices of the ferrous or ferric clusters are accurately reproduced once the two are studied in the same unit cell ( $P^I = 0.54$  eV,  $f_0^I = 0.95$ , and  $\sigma_I = 0.01$  on the ferrous ion and  $P^I = -0.54$  eV,  $f_0^I = 0.28$ , and  $\sigma_I = 0.01$  on the ferric ion). We note that the target occupations for the minority-spin are not chosen exactly one or zero, since the orbital hybridization between the iron  $3d$  orbitals and the lone pairs of the water molecules contributes to the projection onto atomic orbitals (an alternative would be to use projections onto the  $3d$  orbitals or the maximally localized Wannier functions of a solvated iron ion, instead of an isolated atom). When calculating the energy gap, the penalty-functional contributions are taken away from the total energy; in any case, these effects are negligible since these contributions cancel out when calculating energy

differences. Different constraints or penalties have been proposed for density-functional calculations [23–27]; we found our choice particularly robust, but several variations on the theme can be envisioned.

A first, qualitative validation of this penalty functional is performed examining the charge density obtained by subtracting from a calculation with a ferrous and a ferric hexa-aqua ion in the same unit cell that of an isolated ferrous hexa-aqua ion, and that of a ferric hexa-aqua ion (a dielectric continuum surrounds the two clusters to remove long-range electrostatic interactions between them). When the penalty functional is applied, the charge density around the ions reorganizes itself so that it produces a charge density that is the exact superposition of that obtained from the two independent calculations.

We can make our validation quantitative by calculating the energy gap for the system described, using two different penalty-functional calculations that impose to the HOMO electron to localize first on one, then on the other ion. This energy gap can also be calculated exactly with PBE-GGA using the “4-point” approach [28], provided that all long-range electrostatic interactions are screened out. The four calculations involve  $\text{Fe}^{2+}$  in two  $\text{Fe}(\text{H}_2\text{O})_6$  geometries (A and B), and  $\text{Fe}^{3+}$  in the same geometries; the energy gap is  $[E_A(\text{Fe}^{2+}) + E_B(\text{Fe}^{3+}) - E_B(\text{Fe}^{2+}) - E_A(\text{Fe}^{3+})]$ . We choose one configuration in which the hexa-aqua ions are fully relaxed, and three carved out from random steps in the molecular dynamics simulations. The energy gaps we obtained with the penalty functional are 0.632, 0.569, 0.769, and 1.027 eV, in excellent agreement with the “4-point” values of 0.622, 0.542, 0.769, and 1.012 eV. It is worth mentioning that the energy gap is an excited-state property of the system, and thus in principle outside the scope of density-functional theory, which is a ground-state theory. However, since the charge densities of the HOMO and lowest unoccupied molecular orbital (LUMO) do not overlap, we can argue that all that is required is a description of the charge density that is locally correct (the excited state has an electron locally in equilibrium around an iron, oblivious of the other iron ion where it could sit more favorably).

With these tools, we determined the diabatic free-energy surfaces for two iron ions separated by 5.5 Å and solvated in 62 water molecules, in periodic-boundary conditions. 5.5 Å was suggested [4,29] to be the optimal distance for electron transfer. We show our results in Fig. 4, together with a parabolic fit to the data. The reorganization energy ( $\lambda$ ) that we obtain is 2.0 eV [30], in excellent agreement with the experimental value of 2.1 eV [11]. The energy barrier  $\Delta G \approx 0.49$  eV, about a quarter of  $\lambda$ , as expected. We also note that since the structural and electronic configurations of all microstates are available, reaction mechanism (e.g. inner versus outer sphere transfer) can be analyzed in detail by restricting the analysis to all configurations that have a Marcus gap close to zero. Bond-breaking and bond-forming reactions can be followed in detail, or protons can be explicitly introduced [31].

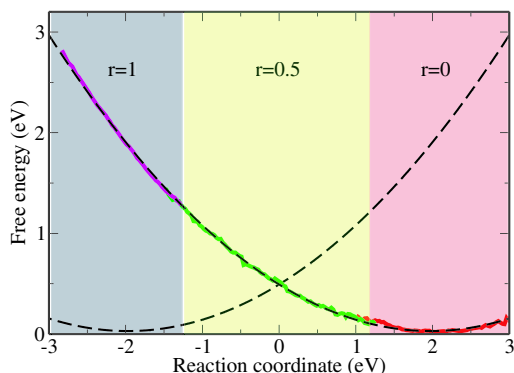


FIG. 4 (color online). Diabatic free-energy surface for ferrous-ferric electron transfer when the two ions are 5.5 Å apart. Different color shades indicate portions of the diabatic surface sampled  $r = 0, 0.5$ , and 1. The right dashed curve is the parabolic fit of the data and the left dashed curve its mirror image.

In conclusion, we have demonstrated how it is possible to obtain Marcus diabatic surfaces from first-principles molecular dynamics. The case when two ions are at a finite distance requires special care in dealing with self-interaction errors and excited-state energies. In response to these challenges, we developed and validated a penalty functional that is able to control the oxidation states of ions, and that describes accurately both the electronic ground state and the first excited state where the electron is transferred to the other ion. This approach can be successfully applied to a wide class of oxidation-reduction reactions, in solution (as it often happens in electrochemistry or biochemistry) or in the solid-state (intervalence charge-transfer).

We gratefully acknowledge support from the Croucher Foundation (P. H.-L. S.), MURI Grant No. DAAD 19-03-1-0169 (N.M.) and the MRSEC Program of the National Science Foundation under Grant No. DMR 02-13282 (P. H.-L. S.). Reference [7] was inspirational in addressing this problem from first principles. The calculations in this work have been performed using the Quantum-ESPRESSO package [32]. Computational facilities have been provided through NSF Grant No. DMR-0414849 and PNNL Grant No. EMSL-UP-9597.

[1] A. Kuznetsov and J. Ulstrup, *Electron Transfer Processes in Chemistry and Biology* (Wiley, New York, 1999).  
 [2] A. Nitzan and M. A. Ratner, *Science* **300**, 1384 (2003).  
 [3] R. A. Marcus and N. Sutin, *Biochim. Biophys. Acta* **881**, 265 (1985).  
 [4] M. D. Newton and N. Sutin, *Annu. Rev. Phys. Chem.* **35**, 437 (1984).  
 [5] A. Warshel and W. W. Parson, *Annu. Rev. Phys. Chem.* **42**, 279 (1991).  
 [6] R. A. Marcus, *Rev. Mod. Phys.* **65**, 599 (1993).

[7] D. Chandler, in *Classical and Quantum Dynamics in Condensed Phase Simulations*, edited by B. J. Berne, G. Ciccotti, and D. F. Coker (World Scientific, Singapore, 1998), pp. 1–66.  
 [8] A. Warshel, *J. Phys. Chem.* **86**, 2218 (1982).  
 [9] A. Warshel, *Nature (London)* **260**, 679 (1976).  
 [10] R. A. Kuharski *et al.*, *J. Chem. Phys.* **89**, 3248 (1988).  
 [11] K. M. Rosso and J. R. Rustad, *J. Phys. Chem. A* **104**, 6718 (2000).  
 [12] A. Warshel and J. Hwang, *J. Chem. Phys.* **84**, 4938 (1986).  
 [13] G. King and A. Warshel, *J. Chem. Phys.* **93**, 8682 (1990).  
 [14] I. Tavernelli, R. Vuilleumier, and M. Sprik, *Phys. Rev. Lett.* **88**, 213002 (2002).  
 [15] J. Blumberger *et al.*, *J. Am. Chem. Soc.* **126**, 3928 (2004).  
 [16] R. Car and M. Parrinello, *Phys. Rev. Lett.* **55**, 2471 (1985).  
 [17] K. Laasonen *et al.*, *Phys. Rev. B* **47**, 10 142 (1993).  
 [18] O, H, and Fe ultrasoft pseudopotentials are from the standard QUANTUM-ESPRESSO distribution (O.pbe-rrkjus.UPF, H.pbe-rrkjus.UPF, and Fe.pbe-sp-van\_mit.UPF). The Fe pseudopotential has 16 valence electrons. The wave functions and charge density cutoffs are 25 and 200 Ryd, respectively. The deuterium mass was used in place of hydrogen mass to allow for a larger time step of integration. The fictitious mass ( $\mu$ ) and the time step are 450 a.u. and 5 a.u., respectively. A Nose-Hoover thermostat was used on the both electrons and ions. The ionic temperature was set at 400 K. See Refs. [33,34].  
 [19] G. Makov and M. C. Payne, *Phys. Rev. B* **51**, 4014 (1995).  
 [20] J. S. Bader and D. Chandler, *J. Phys. Chem.* **96**, 6423 (1992).  
 [21] We note that a GGA + U formulation would require a U of  $\sim 11$  eV to recover localization of charge, but this large U would incorrectly affect the hybridization of the Fe with the nearby water molecules.  
 [22] D. A. Scherlis *et al.*, *J. Chem. Phys.* **124**, 074103 (2006).  
 [23] P. H. Dederichs *et al.*, *Phys. Rev. Lett.* **53**, 2512 (1984).  
 [24] P. H.-L. Sit and N. Marzari, *Bull. Am. Phys. Soc.* **50**, 1289 (2005).  
 [25] M. d’Avezac, M. Calandra, and F. Mauri, *Phys. Rev. B* **71**, 205210 (2005).  
 [26] Q. Wu and T. Van Voorhis, *Phys. Rev. A* **72**, 024502 (2005).  
 [27] J. Behler *et al.*, *Phys. Rev. Lett.* **94**, 036104 (2005); *cond-mat/0605292*.  
 [28] S. F. Nelsen, S. C. Blackstock, and Y. Kim, *J. Am. Chem. Soc.* **109**, 677 (1987).  
 [29] B. L. Tempe, H. L. Friedman, and M. D. Newton, *J. Chem. Phys.* **76**, 1490 (1982).  
 [30] The electrostatic interaction with the periodic images for this unit cell is less than 0.10 eV, assuming very conservatively that only the electrons screen the iron centers. In reality ionic screening of the periodic images dominates even in the product electronic state, leading to negligible electrostatic errors. Also, the pair correlation function of a ferrous or ferric ion in water flattens around 5.5–6 Å and the periodic images of each ion are 10.8 Å apart.  
 [31] J. R. Rustad, K. M. Rosso, and A. R. Felmy, *J. Chem. Phys.* **120**, 7607 (2004).  
 [32] S. Baroni *et al.*, <http://www.quantum-espresso.org>.  
 [33] J. Grossman *et al.*, *J. Chem. Phys.* **120**, 300 (2004).  
 [34] P. H.-L. Sit and N. Marzari, *J. Chem. Phys.* **122**, 204510 (2005).